ACS Catalysis

RESEARCH ARTICLE

pubs.acs.org/acscatalysis

# Complete Oxidation of Formaldehyde at Room Temperature Using $TiO_2$ Supported Metallic Pd Nanoparticles

Haibao Huang and Dennis Y. C. Leung*

Department of Mechanical Engineering, The University of Hong Kong, Pokfulam Road, Hong Kong

**ABSTRACT:** A series of reduced and oxidized $Pd/TiO_2$ catalysts were prepared and used for catalytic oxidation of formaldehyde (HCHO) at room temperature. The reduced catalysts were much more active than the oxidized ones. Nearly 100% HCHO conversion was achieved over the former while it was less than 18% over the latter. Sodium borohydride ($NaBH_4$) reduced $Pd/TiO_2$ catalysts exhibited very high turnover frequencies of HCHO oxidation and kept highly active in the presence of chloride. Strong metal−support interaction, well-dispersed and negatively charged metallic Pd nanoparticles, and rich chemisorbed oxygen are probably responsible for the high catalytic activities over the former. Metallic Pd nanoparticles with a strong capacity for oxygen activation should be the active sites for catalytic oxidation of HCHO.

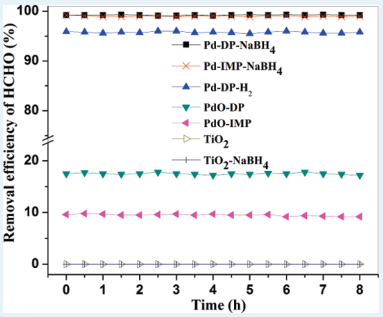


**KEYWORDS:** $Pd/TiO_2$, $NaBH_4$ reduction, HCHO oxidation, room temperature, metallic Pd

## 1. INTRODUCTION

Pd based catalysts have been extensively studied and demonstrated to be highly efficient for the catalytic combustion of volatile organic compounds (VOCs).[1−4] They offer several advantages such as high activity and good thermal stability compared to other precious metal catalysts (such as the Pt and Au based catalysts).[3−6] Moreover, among the precious metals Pd is significantly less expensive and more abundant.[7] Its use in VOCs' destruction is being continuously explored as a potential substitute for the more expensive noble metals.

Nevertheless, deep oxidation of VOCs over Pd catalysts can only occur at high or medium temperature. For example, Pérez-Cadenas et al.[1] reported that complete combustion of xylene was reached over a carbon-coated monoliths supported Pd catalyst in the range between 150 and 180 °C. Álvarez-Galván et al.[8] reported that 100% formaldehyde (HCHO) conversion was achieved over a $Pd/Al_2O_3$ catalyst at 90 °C. An extra heating apparatus is needed for catalytic oxidation, causing higher operating cost and more severe reaction conditions. Therefore, it is highly desirable to destruct VOCs at low temperature, preferably at room temperature as this condition is more environmentally friendly and saves energy.

On the other hand, supported Au and Pt catalysts have exhibited excellent activity for catalytic oxidation of air pollutants at low temperature. For example, Au catalysts possess extraordinary activities for CO oxidation at very low temperature[9−11] and Pt catalysts are found highly effective for HCHO oxidation at room temperature.[12,13] However, Pd catalysts showed nearly no catalytic activity under the same conditions. It is therefore of great significance to investigate the low-temperature characteristics of Pd catalysts.

Even the Pd catalysts have been widely applied for catalytic combustion of VOCs, the effects of Pd oxidation state on the catalytic activity remain controversial.[5,14,15] Many researchers have suggested that the performance of Pd supported catalysts for the oxidation of VOCs is highly dependent on the oxidation state of Pd. Some authors suggest that metallic species ($Pd^0$) are more active than the oxide form ($PdO/Pd^{2+}$) for catalytic oxidation[6,14−16] while the others affirm just the opposite.[17,18] It is generally difficult to distinguish the state of Pd since Pd can readily undergo oxidation/reduction transformations ($Pd \leftrightarrow PdO$) during VOCs catalytic combustion at high temperature, and these transformations might affect the catalytic activity for VOC oxidation.[14,19,20] This may lead to the confusion of the effect of the Pd valence state.

HCHO is one of the most dominant air pollutants in an indoor environment.[21,22] Long-term exposure to indoor air containing even a few ppm of HCHO may cause adverse effects on human health.[23] For indoor air cleaning, low energy demand and low concentration of HCHO strongly require a catalyst to exhibit high activity for its complete oxidation, preferably at ambient temperature.[12,24,25] However, the development of effective catalysts for complete oxidation of low-concentrations of HCHO at ambient temperature is still a challenging subject to be solved.[24,26] Because of the increasing concern on HCHO in the indoor environment, it is of scientific and practical interest to investigate its elimination, particularly at room temperature.

In this work, a series of reduced and oxidized $Pd/TiO_2$ catalysts were prepared and investigated for catalytic oxidation of HCHO at room temperature. The transformations of Pd/PdO would not happen since the Pd state can be kept unchanged at temperature lower than 180 °C.[6,14] It can be easier and clearer to distinguish the catalytic activity of metallic Pd and PdO. The catalysts were characterized and subsequently correlated with their catalytic performances. The $NaBH_4$ reduced Pd catalysts were demonstrated to be highly active for catalytic oxidation of

Received: October 8, 2010
Revised: February 14, 2011
Published: March 03, 2011

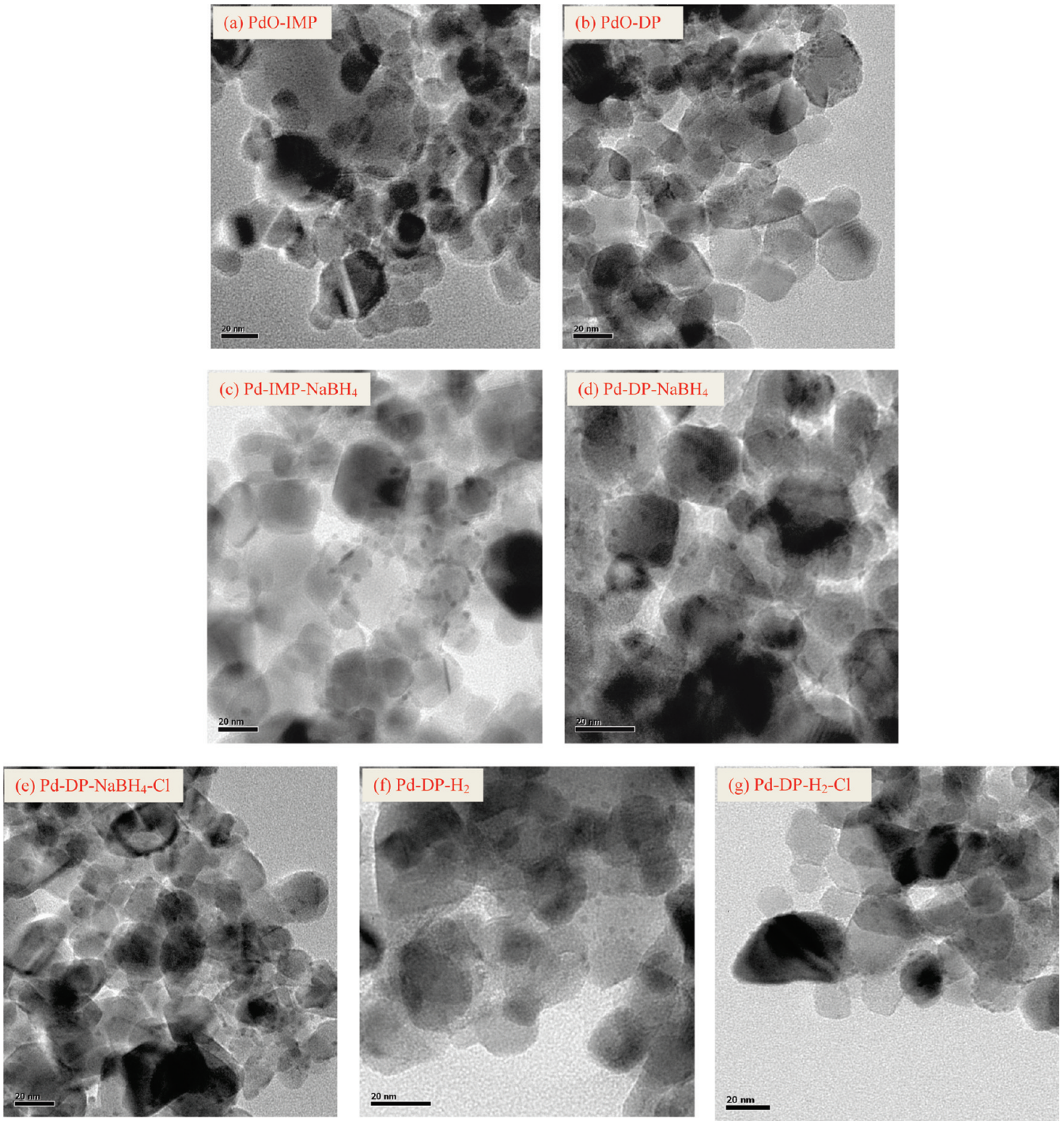


**Figure 1.** TEM micrographs spectra for the 1 wt % $Pd/TiO_2$ catalysts: (a) PdO-IMP, (b) PdO-DP, (c) Pd-IMP-$NaBH_4$, (d) Pd-DP-$NaBH_4$, (e) Pd-DP-$NaBH_4$-Cl, (f) Pd-DP-$H_2$, and (g) Pd-DP-$H_2$-Cl.

HCHO at room temperature for the first time. The possible mechanism leading to the high catalytic activity on the metallic Pd nanoparticles was proposed. This study inspires us to study the low-temperature characteristics of supported Pd catalysts for purification of air pollutants.

## 2. EXPERIMENTAL SECTION

**2.1. Catalyst Preparation.** Both oxidized and reduced 1 wt % $Pd/TiO_2$ catalysts were prepared by using $TiO_2$ powder (P25, Degussa) as the support and $PdCl_2$ as the precursor compound. The oxidized $Pd/TiO_2$ catalysts were synthesized by impregnation and deposition-precipitation methods (denoted as PdO-IMP and PdO-DP, respectively). The PdO-IMP catalyst was prepared as follows: $TiO_2$ support was added into the $PdCl_2$ solution under stirring. After 1 h, the suspension was dried at 80 °C with continuous stirring. The dried samples were further heated at 120 °C for 4 h followed by calcination at 400 °C in air for 4 h, yielding the PdO-IMP catalyst. The PdO-DP catalyst was prepared as follows: $TiO_2$ support was added into the $PdCl_2$


dx.doi.org/10.1021/cs200023p |*ACS Catal.* 2011, 1, 348–354

Table 1. BET Surface Areas, Pd Loading, Pd Dispersion, and TOFs of $Pd/TiO_2$ Together with Pure $TiO_2$

| | | | Pd-IMP-$NaBH_4$ | | | | | |
|---|---|---|---|---|---|---|---|---|
| sample | $TiO_2$ | 1% PdO-IMP | 0.1% | 0.5% | 1% | 1% PdO-DP | 1% Pd-DP- $NaBH_4$ | 1% Pd-DP-$H_2$ |
| BET surface area ($m^2/g$) | 50.8 | 51.7 | 52.3 | 40.6 | 38.6 | 44.3 | 36.1 | 43.5 |
| Pd loading (%) [a] | 0 | 1.16 | 0.08 | 0.52 | 1.05 | 0.92 | 0.99 | 0.97 |
| Pd dispersion (%) | | 17.1 | 23.1 | 30.2 | 28.1 | 45.5 | 31.4 | 68.9 |
| TOF ( $\times 10^{-1}$, $s^{-1}$) [b] | | 0.15 | 2.55 | 3.12 | 3.16 | 0.14 | 3.98 | 1.19 |

[a] Measured by ICP-AES. [b] The TOF is calculated on the basis of surface Pd atoms exposed on the surface from CO-chemisorption.

solution under stirring. After 1 h, a NaOH aqueous solution was added dropwise to the suspension under vigorous stirring until the pH value of the suspension reached 10. The resulting suspension was aged at 60 °C for 2 h, and then washed with distilled water until no chloride anion was detected in the rinsewater with an $AgNO_3$ solution. The resulting precipitate was filtered, dried at 120 °C, and eventually calcined in air at 400 °C for 4 h, yielding the PdO-DP catalyst. The PdO-DP and PdO-IMP catalysts were further treated for 4 h in 20% $H_2$ diluted with argon, resulting in the $H_2$ reduced PdO-DP and PdO-IMP catalysts (denoted as Pd-DP-$H_2$ and Pd-IMP-$H_2$). Impregnation and deposition-precipitation methods were also used to synthesize $NaBH_4$ reduced $Pd/TiO_2$ catalysts. The prepared catalysts were denoted as Pd-IMP-$NaBH_4$ and Pd-DP-$NaBH_4$, respectively. The Pd-IMP-$NaBH_4$ catalyst was prepared with the similar procedures as the PdO-IMP catalyst except that a $NaBH_4$ aqueous solution was added into the suspension of $PdCl_2$ and $TiO_2$ as reducing agent ($NaBH_4$/Pd = 10, molar ratio) under stirring after impregnation for 1 h. The Pd-DP-$NaBH_4$ catalyst was prepared with the similar procedures as the PdO-DP catalyst except that a $NaBH_4$ aqueous solution was added into the suspension as reducing agent ($NaBH_4$/Pd = 10, molar ratio) under stirring after aging. They were directly used for catalytic test after drying without any treatment at high temperature. $H_2$ and $NaBH_4$ reduced $Pd/TiO_2$ catalysts prepared by deposition-precipitation without chloride removal (denoted as Pd-DP-$H_2$-Cl and Pd-DP-$NaBH_4$-Cl) were synthesized to investigate the effect of chloride on catalytic activity. The Pd-DP-$H_2$-Cl and Pd-DP-$NaBH_4$-Cl catalysts were prepared with similar procedures as the Pd-DP-$H_2$ and Pd-DP-$NaBH_4$ catalysts, respectively, except that the dechlorination (by washing with distilled water) was not done in the former catalysts. $NaBH_4$ treated $TiO_2$ (denoted as $TiO_2$-$NaBH_4$) was prepared to examine the effect of support. The reduced $Pd/TiO_2$ was gray in color, as opposed to khaki for the oxidized ones.

**2.2. Catalyst Characterization.** X-ray photoelectron spectroscopy (XPS) measurements of the catalysts were performed with a Physical Electronics 5600 multitechnique system using a monochromatic Al Kα source for the surface composition. The binding energy (BE) was determined by utilizing C1s line as a reference with energy of 285.0 eV. The surface atomic concentration was calculated by using the "Vision Processing" software provided by Kratos. A linear background was used for background subtraction. The relative sensitivity factors (RSF) was 5.356 for Pd, 0.891 for Cl, 2.001 for Ti, and 0.780 for O. Brunauer−Emmett−Teller (BET) surface areas of the samples were measured by $N_2$ adsorption−desorption isotherms at 77 K using a Micromeritics ASAP 2020 instrument. Prior to the measurement, the samples were degassed at 573 K for 2 h. Transmission electron microscopy (TEM) images were recorded on a Tecnai G2 20 microscope operated at 200 kV. The actual Pd loading was analyzed by inductively coupled plasma atomic emission spectroscopy (ICP-AES) (IRIS Intrepid, Thermo Fisher Scientific). The Pd dispersion was determined by pulse CO chemisorption on a Micrometrics AutoChem II 2920 instrument at room temperature, using a thermal conductivity detector (TCD) to monitor CO consumption. A CO/Pd average stoichiometry of 1 has been assumed for the calculation of dispersion.[27,28] Prior to chemisorption, the catalyst was reduced in a stream of 10% $H_2$ diluted with helium at 200 °C for 60 min to remove surface oxygen and then followed by cooling down to room temperature in helium stream.

**2.3. Measurement of Catalytic Activity.** Catalytic oxidation of HCHO was performed in a quartz tubular (i.d. = 6 mm) fixed-bed reactor under atmospheric pressure at ambient temperature (25 ± 1 °C). A 0.5 g portion of the catalyst in 40−60 mesh was loaded in the reactor. An air mixture containing 10 ppm HCHO, water vapor (50% relative humidity) was introduced as the reactants. Gaseous HCHO was generated by passing a stream of zero air through an HCHO solution in an incubator. The air flow was controlled and measured using a series of mass flow controllers (GFC17A, Aalborg, U.S.A.) with an accuracy of ±1.5%. The total flow rate was 1 L/min, corresponding to a gas hourly space velocity (GHSV) of 120,000 $mL/g_{cat}\cdot h$. The HCHO in the air stream were analyzed by an HCHO monitor (Formaldemeter 400, PPM Technology) with 0−50 ppm detection limit and ±2% accuracy. In typical runs, the reaction data were obtained after HCHO oxidation was performed for 2.5 h to achieve steady state. HCHO conversion was calculated as follows:

$$\text{HCHO conversion}(\%) = \frac{[\text{HCHO}]_{\text{in}} - [\text{HCHO}]_{\text{out}}}{[\text{HCHO}]_{\text{in}}} \times 100$$

where $[\text{HCHO}]_{\text{in}}$ and $[\text{HCHO}]_{\text{out}}$ is the HCHO concentration in inlet and outlet gas, respectively.

## 3. RESULTS AND DISCUSSION

**3.1. Structural Features of the Catalysts.** Representative TEM micrographs for the 1 wt % $Pd/TiO_2$ catalysts are presented in Figure.1. It can be found that the TEM micrographs of the reduced catalysts differ from those of the oxidized ones. Small Pd nanoparticles are uniformly present on the reduced catalysts (Figure.1c, 1d, 1e, 1f and 1g). In contrast, no distinguishable crystalline Pd particles are observed over the oxidized ones (Figure 1a and 1b) probably because their size is very small and could not be detected by TEM. However, Pd was identified by ICP-AES and XPS, as listed in Tables 1 and 2, respectively. The actual Pd loading on the $Pd/TiO_2$ catalysts identified by ICP-AES is close to the nominal one (i.e., 1 wt %). Pd catalysts prepared by different methods exist differently in terms of crystal

**Table 2. XPS Data for the 1 wt % Pd/$TiO_2$ Catalysts**

| | BE, eV | | | | | surface content, wt% | |
|---|---|---|---|---|---|---|---|
| catalyst | Pd $3d_{5/2}$ | $O_{II}$ ($O_I$) | Ti $2p_{3/2}$ | Cl $2p_{3/2}$ | surface atomic ratio ($O_{II}$ /$O_I$) [a] | Pd | Cl |
| PdO-IMP | 336.2 | 532.2 (530.3) | 459.1 | 198.8 | 0.033 | 2.82 | 1.03 |
| Pd-IMP-$NaBH_4$ | 334.2 | 531.4 (529.5) | 458.3 | 198.7 | 0.25 | 1.45 | 2.26 |
| PdO-DP | 336.2 | 531.4 (529.5) | 458.3 | | 0.11 | 1.56 | n. d.[b] |
| Pd-DP-$NaBH_4$ | 334.6 | 531.4 (529.5) | 458.3 | | 0.27 | 1.52 | n. d.[b] |
| Pd-DP-$H_2$ | 335.1 | 531.9 (530.0) | 458.8 | | 0.073 | 1.84 | n. d.[b] |

[a] Calculated from the corresponding areas of fitted peaks done by XPSPEAK 4.1 with Shirley background. [b] n. d.: not detected.

structure. Reduction treatment promoted the formation of Pd clusters. The Pd particles over the reduced 1 wt % Pd/$TiO_2$ catalysts are well dispersed and have a homogeneous size of only about 3 nm on the Pd-IMP-$NaBH_4$, 2.5 nm on the Pd-DP-$NaBH_4$, and 2.2 nm on the Pd-DP-$H_2$. The Pd nanoparticles size is about 2.4 nm on the Pd-DP-$NaBH_4$-Cl and 2.6 nm on the Pd-DP-$H_2$-Cl, which is close to that on the corresponding dechlorinated Pd/$TiO_2$ catalysts, indicating that the presence of chloride did not significantly promote the growth of Pd particles.

The BET surface areas of the Pd/$TiO_2$ catalysts together with pure $TiO_2$ are summarized in Table 1. The surface area of the PdO-IMP catalyst kept almost the same as that of pure $TiO_2$. However, they significantly dropped on the other Pd/$TiO_2$ catalysts, especially on the $NaBH_4$ reduced ones. The decrease of BET surface area on the precipitated catalysts was probably because the NaOH used for the precipitation affected the physical properties of the catalysts (such as pore volume and pore size). NaOH deposited on the outer surface of the support probably fills its pores of $TiO_2$, resulting in the decrease of BET surface. As for the $NaBH_4$ reduced catalysts, the $NaBH_4$ affected and changed the surface area of $TiO_2$. NaOH was formed as $NaBH_4$ was added into the suspension. The pH value of suspension was increased from 1.95 to 9.68 after $NaBH_4$ reduction during the preparation of 1 wt % Pd-IMP-$NaBH_4$. The BET surface area of the 0.1 wt % Pd-IMP-$NaBH_4$ is 52.3 $m^2$/g, which is close to that of pure $TiO_2$ (see Table 1). The change of BET surface area of the 0.1 wt % Pd-IMP-$NaBH_4$ is not significant probably because of its low Pd loading and small dosage of $NaBH_4$.

**3.2. Catalytic Activity.** Figure.2 shows the time dependence of HCHO removal efficiency for the 1 wt % Pd/$TiO_2$ catalysts together with pure $TiO_2$ and $TiO_2$-$NaBH_4$ at ambient temperature. Pure $TiO_2$ and $TiO_2$-$NaBH_4$ showed no activity for HCHO oxidation, indicating that the removal of HCHO by the supports can be excluded. It can be found that the activities of the Pd/$TiO_2$ catalysts were greatly influenced by the reduction treatment. Only 9.2% and 17.6% HCHO conversion was obtained over the PdO-IMP and PdO-DP catalyst, respectively. This result is in agreement with the low activity for HCHO oxidation on the oxidized Pd catalysts observed in a previous study.[13,22] The PdO-DP catalyst achieved a higher HCHO conversion than the PdO-IMP catalyst because of its higher Pd dispersion which resulted in more active sites. However, their turnover frequencies (TOFs) are similar (see Table 1). Compared with the oxidized Pd/$TiO_2$ catalysts, the reduced ones obtained much higher catalytic activity. It can be found from Figure 2 that HCHO conversion exceeded 95.5% on the reduced Pd/$TiO_2$ catalysts.

Comparing Table 1 with Figure 2, no simple correlation could be found between the activity and the BET surface area of the catalysts. In addition, the discrepancy of particles size and Pd dispersion also cannot explain well the big difference in catalytic activity on the Pd/$TiO_2$ catalysts. As described previously, the oxidized Pd/$TiO_2$ catalysts possessed smaller Pd particles in comparison with the reduced ones; however, their HCHO conversion is much lower than the latter. The activities of Pd catalysts for catalytic oxidation of VOCs were regarded to be highly dependent on the oxidation state of Pd.[5] The XPS analysis was carried out to identify the oxidation states and surface concentration of the Pd particles. XPS spectra and data for the 1 wt % Pd/$TiO_2$ catalysts are shown in Figure 3 and listed in Table 2, respectively. The peaks of $3d_{5/2}$ over the PdO-IMP and PdO-DP catalysts are centered at 336.2 eV, which are very close to the BE of $Pd^{2+}$, and far from the BE of $Pd^0$.[14] They are shifted to a lower BE of 334.2 eV on the Pd-IMP-$NaBH_4$, 334.6 eV on the Pd-DP-$NaBH_4$, and 335.1 eV on the Pd-DP-$H_2$, which corresponds to metallic Pd.[29] Pd was reduced into metallic state after reduction.

It can be found from Table 2 that the surface Pd mass concentration is 2.82% on the PdO-IMP catalyst, 1.45% on Pd-IMP-$NaBH_4$, 1.56% on the PdO-DP, 1.52% on the Pd-DP-$NaBH_4$, and 1.84% on the Pd-DP-$H_2$, all of which are larger than the actual Pd loading determined by ICP-AES which is close to 1 wt % (see Table 1). The high surface Pd concentration on the PdO-IMP catalyst is probably due to the weak interaction of Pd precursor and the support, leading to the enrichment of Pd species on the surface of support. The Pd dispersion of the PdO-IMP is only 17.1%, as shown in Table 1. The surface Pd concentration was greatly decreased on the precipitated Pd catalysts, probably indicating that the Pd enrichment was decreased and the Pd dispersion was improved. As observed in Table 1, the precipitated and $NaBH_4$ reduced Pd/$TiO_2$ catalysts possessed much higher Pd dispersion than the PdO-IMP. The improved Pd dispersion probably results from strong interaction of the Pd precursor and the support during the deposition-precipitation process. The deposition-precipitation is concurrent during the preparation of the Pd-IMP-$NaBH_4$ since NaOH was formed as $NaBH_4$ was added into the suspension, as previously described. Well-dispersed Pd nanoparticles located on the surface of supports can provide active sites and are favorable for reaction. The TOFs of HCHO oxidation on different Pd/$TiO_2$ catalysts are listed in Table 1. It is $3.16 \times 10^{-1}$ $s^{-1}$ for the 1 wt % Pd-IMP-$NaBH_4$, $3.98 \times 10^{-1}$ $s^{-1}$ for the 1 wt % Pd-DP-$NaBH_4$, and $1.19 \times 10^{-1}$ $s^{-1}$ for the 1 wt % Pd-DP-$H_2$, whereas it is less than $0.15 \times 10^{-1}$ $s^{-1}$ for the oxidized ones. The reduced Pd/$TiO_2$ catalysts achieved much higher TOFs than the oxidized ones. These results also suggest that the Pd oxidation state is crucial to the catalytic activity of Pd/$TiO_2$, and metallic Pd rather


dx.doi.org/10.1021/cs200023p |*ACS Catal.* 2011, 1, 348–354

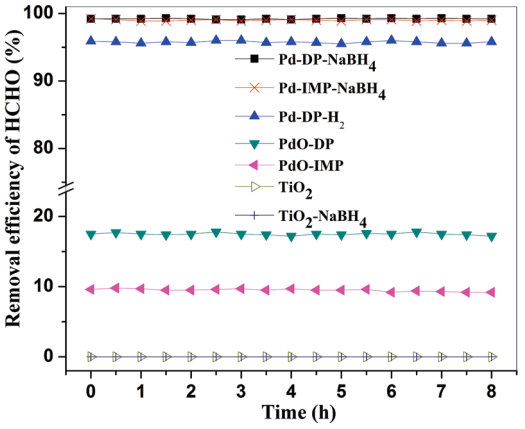


**Figure 2.** HCHO removal efficiency over the 1 wt % $Pd/TiO_2$ catalysts, pure $TiO_2$ and $TiO_2$-$NaBH_4$ (HCHO concentration = 10 ppm, relative humidity = 50% and GHSV = 120,000 mL/$g_{cat}$·h).

than cationic Pd is the active site for HCHO oxidation. This conclusion is consistent with those in previous study.[6,14−16]

Catalytic activity of $Pd/TiO_2$ catalysts was also greatly affected by the reduction methods. As shown in Table 1, $NaBH_4$ reduced $Pd/TiO_2$ catalysts showed higher catalytic activity than the $H_2$ reduced one. The TOF of 1 wt % Pd-DP-$NaBH_4$ is more than 3 times of that of the 1 wt % Pd-DP-$H_2$. It can be found from Figure 3a that the Pd $3d_{5/2}$ showed a significant negative shift of 0.9 and 0.5 eV on the Pd-IMP-$NaBH_4$ and Pd-DP-$NaBH_4$, respectively, with respect to 335.1 eV of the Pd-DP-$H_2$, indicating that Pd nanoparticles are negatively charged and strong metal−support interaction (SMSI) is present on the $NaBH_4$ reduced $Pd/TiO_2$ catalysts. The SMSI was also confirmed by the BE shift of O 1s and Ti 2p on them. As shown in Table 2, the main peaks of O 1s and Ti $2p_{3/2}$ on the Pd-DP-$H_2$ are located at 530.0 and 458.8 eV, respectively, which are ascribed to lattice oxygen and $Ti^{4+}$ of $TiO_2$.[30] In comparison, the corresponding peaks both made a negative shift of about 0.5 eV over the Pd-IMP-$NaBH_4$ and Pd-DP-$NaBH_4$. It can be found that the PdO-DP catalyst also made a similar shift of Ti 2p as the $NaBH_4$ reduced Pd catalysts did. This strong interaction turned weaker after $H_2$ reduction at high temperature. The shift of Ti $2p_{3/2}$ peak to a lower energy suggests that partial $Ti^{4+}$ probably exists in the state of $TiOx$ ($x < 2$), on which the chemisorption of oxygen can be enhanced because of the presence of oxygen vacancies.[31,32] It was reported that negatively charged noble metal nanoparticles also show enhanced $O_2$ adsorption since the donation from the metal to the antibonding $\pi^*$ orbital of $O_2$ is enhanced.[31,32] This chemisorbed oxygen was confirmed by O 1s XPS spectra, as shown in Figure 3b. O 1s spectra exhibit two peaks: a main peak at 529.5 eV for the Pd-IMP-$NaBH_4$, Pd-DP-$NaBH_4$, and PdO-DP catalysts, at 530.0 eV for the Pd-DP-$H_2$ and at 530.3 eV for the PdO-IMP catalyst (named $O_I$), and a corresponding shoulder peak at 531.4, 531.9, and 532.2 eV (named $O_{II}$). These results indicate two types of oxygen specie exist on the $Pd/TiO_2$ catalysts. $O_I$ can be attributed to lattice oxygen for $TiO_2$ and $O_{II}$ should be ascribed to the chemisorbed oxygen.[29,33−35] The adsorbed oxygen was not solely on Pd. Instead, a large proportion of oxygen must have been located on the support.[36] $O_{II}$ might possess high mobility and be deeply involved in the redox cycles of HCHO oxidation. It also can be observed from Figure 3b that the $O_{II}$ peaks over the $NaBH_4$ reduced $Pd/TiO_2$ catalysts are significantly stronger than that on the

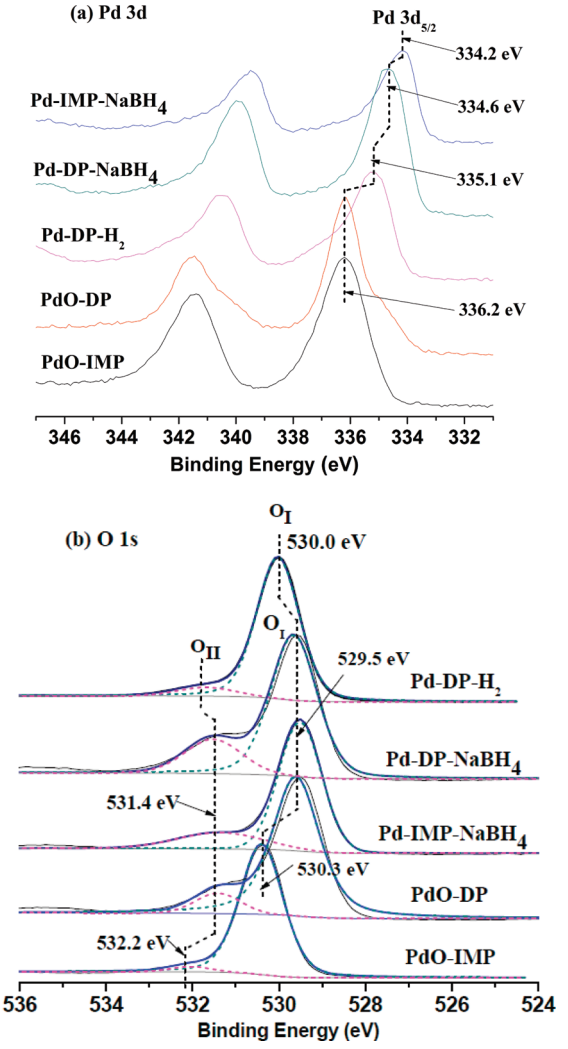


**Figure 3.** XPS spectra of the oxidized and reduced 1 wt % $Pd/TiO_2$ samples: (a) Pd 3d and (b) O 1s.

$H_2$ reduced one. The $O_{II}$ content was affected by the SMSI effect, reduction methods as well as Pd oxidation state. Comparing Table 2 with Figure 3, it can be found that the stronger effect of SMSI on the Pd-IMP-$NaBH_4$, Pd-DP-$NaBH_4$, and PdO-DP corresponds to the higher $O_{II}$ intensity. The $O_{II}/O_I$ ratio was calculated from the corresponding peak areas, and the results were listed in Table 2. Comparing Table 1 with Table 2, it can be found that the TOFs are greatly affected by the $O_{II}/O_I$ ratio. The $NaBH_4$ reduced $Pd/TiO_2$ catalysts with higher $O_{II}/O_I$ ratio obtained higher TOF than the $H_2$ reduced one. The Pd-DP-$NaBH_4$ catalyst has about 2.5 times of $O_{II}/O_I$ ratio but more than 20 times of TOF compared with that of the PdO-DP (Table 1). Therefore, the capability of the $Pd/TiO_2$ catalysts to activate the chemisorbed oxygen is also a critical factor determining their catalytic activity besides of the capacity for generation of chemisorbed oxygen. The chemisorbed oxygen can be more easily activated by metallic Pd than cationic Pd. Metallic Pd nanoparticles with a very strong capacity for oxygen activation were the active sites for catalytic oxidation of HCHO. The activated oxygen will be involved in HCHO oxidation. This conclusion is consistent with that derived from CO oxidation over Au nanoparticles at low temperature, for which metallic Au particles appear to take part in the activation of molecular


dx.doi.org/10.1021/cs200023p |ACS Catal. 2011, 1, 348–354

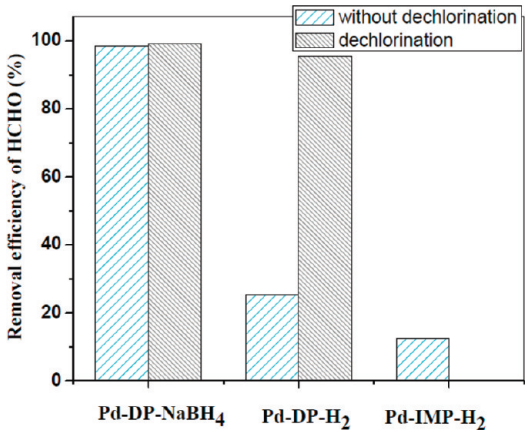


**Figure 4.** Effect of dechlorination on HCHO conversion over the reduced 1 wt % $Pd/TiO_2$ catalysts (HCHO concentration = 10 ppm, relative humidity = 50% and GHSV = 120, 000 $mL/g_{cat}\cdot h$).

oxygen.[37] Strong metal−support interaction negatively charged metallic Pd nanoparticles, and rich chemisorbed oxygen are probably responsible for the high catalytic activity over the $NaBH_4$ reduced catalysts in comparison with the oxidized and $H_2$ reduced ones.

The residual chloride was identified on the 1 wt % Pd-IMP-$NaBH_4$ and 1 wt % PdO-IMP catalysts by XPS. As shown in Table 2, the Cl $2p_{3/2}$ peak on them is centered at 198.8 and 198.7 eV, respectively, corresponding to $Cl^-$.[38] The surface chloride concentration on the 1 wt % Pd-IMP-$NaBH_4$ catalyst (2.26 wt %) is much larger than that on the 1 wt % PdO-IMP catalyst (1.03 wt %), indicating that chloride was accumulated on the surface of catalyst after $NaBH_4$ reduction. However, the former obtained much higher catalytic activity than the latter. Moreover, it achieved higher TOF than the 1 wt % PdO-DP and 1 wt % PdO-DP-$H_2$, on which no residual chloride was detected (Table 2). The results indicated that the $NaBH_4$ reduced $Pd/TiO_2$ catalysts kept highly active in the presence of chloride in this reaction. Figure 4 shows the effect of dechlorination on HCHO conversion over the reduced $Pd/TiO_2$ catalysts. It can be found that HCHO conversion is 95.5% over the Pd-DP-$H_2$ while it dropped to 25.4% over the Pd-DP-$H_2$-Cl, indicating that the $Pd/TiO_2$ catalysts were seriously poisoned in the presence of chloride during the $H_2$ reduction at high temperature. As observed in Figure 1, the Pd particle size did not significantly change in the presence of chloride during the preparation, and the size effect should not be responsible for the poisoning on the Pd-DP-$H_2$-Cl. The low catalytic activity was also observed on the Pd-IMP-$H_2$ with HCHO conversion of only 12.5%. However, the HCHO conversion was only slightly decreased on the Pd-DP-$NaBH_4$-Cl compared with the Pd-DP-$NaBH_4$. The results also suggested the $NaBH_4$ reduced $Pd/TiO_2$ catalysts kept highly active in the presence of chloride. The discrepancy in susceptibility to chloride inhibition on different catalysts is probably caused by different conditions of preparation and reducing agents used. However, more work is needed to find out the mechanism leading to the extraordinary stability of the $NaBH_4$ reduced $Pd/TiO_2$ catalysts in the presence of chlorine in the future.

## 4. CONCLUSION

Highly active $Pd/TiO_2$ catalysts were prepared by $NaBH_4$ reduction in a very simple process with mild conditions. Well-dispersed Pd nanoparticles with very small size (less than 3 nm) were obtained on them. Nearly 100% HCHO conversion was achieved over the $NaBH_4$ reduced 1 wt % $Pd/TiO_2$ catalysts while it was less than 18% over the oxidized ones at room temperature. $NaBH_4$ reduced $Pd/TiO_2$ catalysts showed high TOFs of HCHO oxidation and kept highly active in the presence of chloride. SMSI, negatively charged metallic Pd nanoparticles, and rich chemisorbed oxygen are probably responsible for the high catalytic activity on the former. Metallic Pd nanoparticles with a strong capacity for oxygen activation should be the active sites for catalytic oxidation of HCHO. We successfully extended the complete catalytic oxidation of HCHO over Pd catalysts from medium temperature to room temperature.

## AUTHOR INFORMATION

### Corresponding Author

*Phone: (852)2859-7911. Fax: (852)2858-5415. E-mail: ycleung@hku.hk.

### Funding Sources

The authors gratefully acknowledge the financial supports from the CRCG of the University of Hong Kong (Grant 200907176159).

## REFERENCES

(1) Pérez-Cadenas, A. F.; Kapteijn, F.; Moulijn, J. A.; Maldonado-Hódar, F. J.; Carrasco-Marín, F.; Moreno-Castilla, C. *Carbon* **2006**, *44* (12), 2463–2468.
(2) Dégé, P.; Pinard, L.; Magnoux, P.; Guisnet, M. *Appl. Catal., B* **2000**, *27* (1), 17–26.
(3) Zuo, S.; Huang, Q.; Zhou, R. *Catal. Today* **2008**, *139* (1−2), 88–93.
(4) Giraudon, J. M.; Elhachimi, A.; Wyrwalski, F.; Siffert, S.; Aboukaï, A.; Lamonier, J. F.; Leclercq, G. *Appl. Catal., B* **2007**, *75* (3−4), 157–166.
(5) Kim, S. C.; Shim, W. G. *Appl. Catal., B* **2009**, *92* (3−4), 429–436.
(6) Huang, S.; Zhang, C.; He, H. *Catal. Today* **2008**, *139* (1−2), 15–23.
(7) González, J. R.; Aranzabal, A.; Gutiérrez-Ortiz, J. I.; López-Fonseca, R.; Gutiérrez-Ortiz, M. A. *Appl. Catal., B* **1998**, *19* (3−4), 189–197.
(8) Álvarez-Galván, M. C.; Pawelec, B.; de la Peña O'Shea, V. A.; Fierro, J. L. G.; Arias, P. L. *Appl. Catal., B* **2004**, *51* (2), 83–91.
(9) Haruta, M.; Yamada, N.; Kobayashi, T.; Iijima, S. *J. Catal.* **1989**, *115* (2), 301–309.
(10) Herzing, A. A.; Kiely, C. J.; Carley, A. F.; Landon, P.; Hutchings, G. J. *Science* **2008**, *321* (5894), 1331–1335.
(11) Bulushev, D. A.; Yuranov, I.; Suvorova, E. I.; Buffat, P. A.; Kiwi-Minsker, L. *J. Catal.* **2004**, *224* (1), 8–17.
(12) Zhang, C. B.; He, H.; Tanaka, K. *Appl. Catal., B* **2006**, *65* (1−2), 37–43.
(13) Zhang, C.; He, H. *Catal. Today* **2007**, *126* (3−4), 345–350.
(14) Ihm, S.-K.; Jun, Y.-D.; Kim, D.-C.; Jeong, K.-E. *Catal. Today* **2004**, *93*−*95*, 149–154.
(15) Cordi, E. M.; Falconer, J. L. *J. Catal.* **1996**, *162* (1), 104–117.
(16) Shim, W. G.; Lee, J. W.; Kim, S. C. *Appl. Catal., B* **2008**, *84* (1−2), 133–141.
(17) Su, S. C.; Carstens, J. N.; Bell, A. T. *J. Catal.* **1998**, *176* (1), 125–135.
(18) Farrauto, R. J.; Lampert, J. K.; Hobson, M. C.; Waterman, E. M. *Appl. Catal., B* **1995**, *6* (3), 263–270.
(19) Thevenin, P. O.; Alcalde, A.; Pettersson, L. J.; Järå, S. G.; Fierro, J. L. G. *J. Catal.* **2003**, *215* (1), 78–86.
(20) Lyubovsky, M.; Pfefferle, L. *Catal. Today* **1999**, *47* (1−4), 29–44.

(21) Wang, L.; Sakurai, M.; Kameyama, H. *J. Hazard. Mater.* **2009**, *167* (1−3), 399–405.
(22) Peng, J. X.; Wang, S. D. *Appl. Catal., B* **2007**, *73* (3−4), 282–291.
(23) Sekine, Y. *Atmos. Environ.* **2002**, *36* (35), 5543–5547.
(24) Tang, X. F.; Chen, J. L.; Huang, X. M.; Xu, Y.; Shen, W. J. *Appl. Catal., B* **2008**, *81* (1−2), 115–121.
(25) Wang, L. F.; Zhang, Q.; Sakurai, M.; Kameyama, H. *Catal. Commun.* **2007**, *8* (12), 2171–2175.
(26) Zhang, C. B.; He, H.; Tanaka, K. *Catal. Commun.* **2005**, *6* (3), 211–214.
(27) Fox, E. B.; Velu, S.; Engelhard, M. H.; Chin, Y.-H.; Miller, J. T.; Kropf, J.; Song, C. *J. Catal.* **2008**, *260* (2), 358–370.
(28) Zhu, Q. C.; Shen, B. X.; Ling, H.; Gu, R. *J. Hazard. Mater.* **2010**, *175* (1−3), 646–650.
(29) Wu, Z.; Sheng, Z.; Liu, Y.; Wang, H.; Tang, N.; Wang, J. *J. Hazard. Mater.* **2009**, *164* (2−3), 542–548.
(30) Chen, X.; Burda, C. *J. Phys. Chem. B* **2004**, *108* (40), 15446–15449.
(31) Arrii, S.; Morfin, F.; Renouprez, A. J.; Rousset, J. L. *J. Am. Chem. Soc.* **2004**, *126* (4), 1199–1205.
(32) Hutchings, G.J. *Dalton Trans.* **2008**, *41*, 5523–5536.
(33) Yang, S.; Zhu, W.; Jiang, Z.; Chen, Z.; Wang, J. *Appl. Surf. Sci.* **2006**, *252* (24), 8499–8505.
(34) Cao, J. L.; Shao, G. S.; Ma, T. Y.; Wang, Y.; Ren, T. Z.; Wu, S. H.; Yuan, Z. Y. *J. Mater. Sci.* **2009**, *44* (24), 6717–6726.
(35) Zhou, L.; Deng, J.; Zhao, Y.; Liu, W.; An, L.; Chen, F. *Mater. Chem. Phys.* **2009**, *117* (2−3), 522–527.
(36) Liu, L.; Zhou, F.; Wang, L.; Qi, X.; Shi, F.; Deng, Y.; Low-temperature, C. O. *J. Catal.* **2010**, *274* (1), 1–10.
(37) Weiher, N.; Beesley, A. M.; Tsapatsaris, N.; Delannoy, L.; Louis, C.; van Bokhoven, J. A.; Schroeder, S. L. M. *J. Am. Chem. Soc.* **2007**, *129* (8), 2240–2241.
(38) Alfonso, G.; del Valle, M. A.; Soto, G. M.; Cotarelo, M. A.; Quijada, C.; Vázquez, J. L. *Polym. Bull.* **2006**, *56* (2), 201–210.